
Contrastive Multi-Modal Clustering

Jie Xu^{1†}, Huayi Tang^{1†}, Yazhou Ren^{1*}, Xiaofeng Zhu¹, Lifang He²

¹University of Electronic Science and Technology of China

²Lehigh University

Abstract

Multi-modal clustering, which explores complementary information from multiple modalities or views, has attracted people’s increasing attentions. However, existing works rarely focus on extracting high-level semantic information of multiple modalities for clustering. In this paper, we propose Contrastive Multi-Modal Clustering (CMMC) which can mine high-level semantic information via contrastive learning. Concretely, our framework consists of three parts. (1) Multiple autoencoders are optimized to maintain each modality’s diversity to learn complementary information. (2) A feature contrastive module is proposed to learn common high-level semantic features from different modalities. (3) A label contrastive module aims to learn consistent cluster assignments for all modalities. By the proposed multi-modal contrastive learning, the mutual information of high-level features is maximized, while the diversity of the low-level latent features is maintained. In addition, to utilize the learned high-level semantic features, we further generate pseudo labels by solving a maximum matching problem to fine-tune the cluster assignments. Extensive experiments demonstrate that CMMC has good scalability and outperforms state-of-the-art multi-modal clustering methods.

1 Introduction

In real-world application scenarios, people need to deal with more and more tasks of multi-modal or multi-view data [1, 2, 3, 4, 5]. For examples, visual and textual information can be combined to better describe the webpages, image information can be represented by different descriptors such as SIFT and LBP. Therefore, as a fundamental research topic in machine learning and data science communities, multi-modal clustering has attracted more and more attentions in recent years [6, 7, 8, 9, 10]. Multiple modalities contain complementary information that can be used to mine more comprehensive cluster patterns, which is the rationale for using multi-modal data to improve the clustering performance.

Existing multi-modal clustering (MMC) methods can be roughly divided into the following four categories. The most widely studied category of MMC belongs to subspace clustering [11, 12, 13], which focuses on learning a common subspace representation for multiple modalities or multiple views. The second MMC category is based on the matrix factorization technique [14, 15, 16] that is formally equivalent to the relaxation of K -means [17]. The third category is graph-based MMC [6, 18, 19], where graph structure is conducive to keep the adjacency relationship between samples to find the cluster patterns. Recently, with the rapid development of deep learning, multi-modal clustering combined with deep models [7, 8, 10, 20, 21, 22] has gradually become a popular trend in the community, which can be summarized as the fourth category of MMC.

Although important progress has been achieved in many fields with the existing MMC approaches, more or less, their performance is limited due to the following drawbacks. Traditional MMC methods are implemented with shallow models or linear embedding, leading to poor clustering performance on real-world complex data. Many MMC methods suffer from certain sensitive hyperparameters,

[†]Equal contribution. *Corresponding author. Email: yazhou.ren@uestc.edu.cn

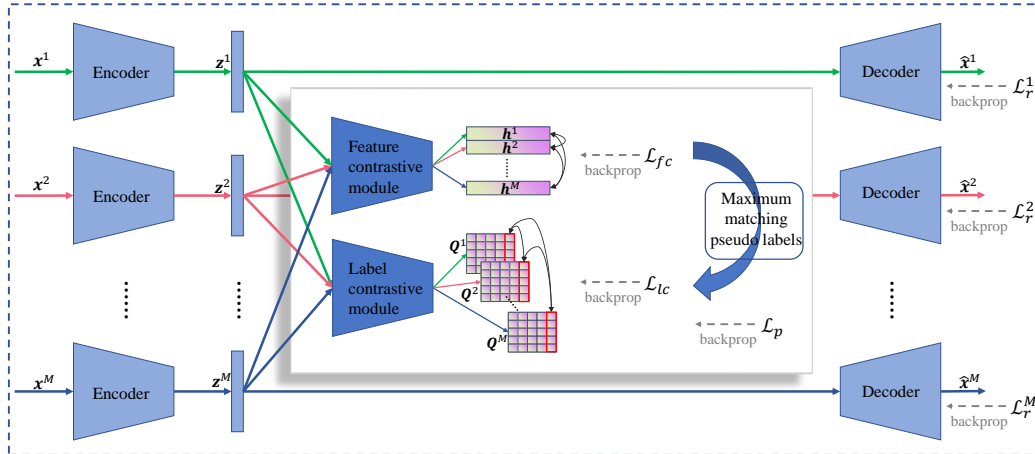


Figure 1: The framework of CMMC. A feature contrastive module is proposed to learn common high-level semantic features $\{h^m\}_{m=1}^M$ of all modalities, while M autoencoders are introduced to maintain the diversity of low-level latent features $\{z^m\}_{m=1}^M$. A label contrastive module is used for learning consistent cluster predictions $\{Q^m\}_{m=1}^M$, which are fine-tuned by the pseudo labels generated from the high-level semantic features.

which make the algorithms perform unstably on different datasets. High computational complexity of some methods reduces their feasibility on increasing data size. In addition, it is a long-standing problem to effectively mine consistent and complementary information, especially for the high-level semantic information among multiple modalities.

It is a basic assumption that multiple modalities have common and high-level semantic representations. For an intuitive example, the image and text about “cats” are much different, but their high-level features should represent the same semantic information, i.e., the cat. To improve clustering performance by mining multi-modal high-level semantic information, we propose contrastive multi-modal clustering (CMMC) whose framework is shown in Figure 1. Concretely, based on contrastive learning, the feature contrastive loss \mathcal{L}_{fc} is optimized to learn common high-level semantic features among all modalities, which is theoretically equivalent to maximizing their mutual information. The label contrastive loss \mathcal{L}_{lc} is also optimized to obtain the consistent cluster assignments of multiple modalities. Meanwhile, the reconstruction losses $\{\mathcal{L}_r^m\}_{m=1}^M$ of autoencoders are optimized, so as to maintain the diversity of the latent features, which are treated as low-level latent features that can contain more complementary information. After that, the high-level semantic features are merged to calculate the pseudo labels via a global maximum match, which are used to fine-tune the cluster assignments by optimizing the cross-entropy loss \mathcal{L}_p . This novel multi-modal contrastive learning framework is scalable with the number of modalities, whose contributions are summarized as three aspects:

- We propose a multi-modal contrastive learning method to obtain common high-level semantic features and consistent cluster assignments of all modalities. The high-level semantic features enjoy good manifolds and are conducive to promote clustering performance.
- We consider both multi-modal consistency and diversity, so the proposed framework distinguishes between high-level semantic features and low-level latent features. To our knowledge, this could be the first work about contrastive clustering with multiple modalities.
- The proposed method has the advantages of scalability and robustness. Besides, this deep model is useful for dealing with large-scale multi-modal data. Extensive experiments on different types of datasets demonstrate that it achieves state-of-the-art clustering performance.

2 Related work

Multi-modal clustering. We introduce four categories of works about multi-modal or multi-view clustering. (1) Since subspace clustering is one of the most popular clustering methods, much attention is paid to multi-modal subspace clustering in the past decade. For instance, the traditional subspace clustering was extended in [23], where the authors presented a diversity-induced multi-

modal clustering method. A recent work [24] proposed a multi-modal subspace clustering method, in which a consistent representation and a set of specific representations are simultaneously learned. (2) Some multi-modal clustering methods apply non-negative matrix factorization to mine a common latent factor among all modalities of data. For example, Cai *et al.* [25] introduced a shared clustering indicator matrix for multiple modalities and handled a constrained matrix factorization problem. (3) Graph-based methods, such as [6, 18, 19], are also proposed for multi-modal clustering. More instance-level relationships can be preserved in graph structures, which is an advantage of this category of approaches. (4) Recently, deep multi-modal clustering has been exploited increasingly [8, 9, 10, 21], which utilizes the excellent feature transformation capability of deep neural networks. In [7], for instance, the authors leveraged autoencoders and adversarial training to learn the latent distribution of data. Xu *et al.* [20] proposed a collaborative training method to train all modalities and explicitly achieve consistent cluster predictions.

Contrastive learning. Unsupervised representation learning [26] aims to learn the representation, which is a transformation of high-dimensional or complex data that can make subsequent tasks solving easier. Contrastive learning [27] is an attention-getting unsupervised representation learning method, with the idea that maximizing the similarities of positive pairs while minimizing that of negative pairs in a feature space. This learning paradigm has lately achieved promising performance in computer vision, such as [28, 29]. For example, a one-stage online image clustering method was proposed in [30], which explicitly performs contrastive learning in the instance-level and cluster-level. For multi-modal learning, there are also some works based on contrastive learning [31, 32, 33, 34]. For instance, Tian *et al.* [31] investigated a contrastive multi-modal coding framework to capture underlying scene semantics. In [32], the authors developed a multi-modal representation learning method to tackle graph classification via contrastive learning.

The differences between this work and existing studies are as follows. Existing contrastive learning based methods mainly handle single-modal or two-modal problems. To our knowledge, however, this work could be the first research about multi-modal contrastive clustering. Besides, when learning consistency from different modalities, little attention has been paid to losing complementary information caused by performing contrastive learning directly in the feature space. In contrast, our method distinguishes between high-level and low-level features. Specifically, it leverages autoencoders to maintain the diversity and complementary information among multiple modalities, and introduces feature and label contrastive modules to indirectly achieve the consistency of high-level semantic features and cluster assignments. In this way, the high-level features can provide a positive feedback for improving clustering performance.

3 Contrastive Multi-Modal Clustering

Problem formulation. Given a dataset $\mathcal{D} = \{\mathbf{x}_i^m\}_{i=1, \dots, N}^{m=1, \dots, M}$ including N instances of M modalities, where $\mathbf{x}_i^m \in \mathbb{R}^{D_m}$ denotes the D_m -dimensional instance from the m -th modality, multi-modal clustering aims to partition the instances into K clusters without using any label information.

3.1 Multi-modal contrastive learning

The proposed framework is shown in Figure 1. In this section, we introduce its components and the corresponding motivations.

Multi-modal autoencoders. Autoencoder [35] can implement nonlinear mapping by learning a latent feature space between the input and output. Without loss of generality, different modalities of an instance are different in forms or dimensions. Therefore, for each modality, we adopt a deep autoencoder to learn the latent features that are convenient for clustering. Let $E^m(\mathbf{x}^m; \theta^m)$ and $D^m(\mathbf{z}^m; \phi^m)$ denote the encoder and decoder, where θ^m and ϕ^m are network parameters. $\mathbf{z}_i^m = E^m(\mathbf{x}_i^m) \in \mathbb{R}^L$ denotes the L -dimensional latent feature. For the m -th modality, the reconstruction loss \mathcal{L}_r^m between input and output is optimized to map the data into latent features. The total reconstruction loss is formulated as:

$$\mathcal{L}_r = \sum_{m=1}^M \mathcal{L}_r^m = \sum_{m=1}^M \sum_{i=1}^N \|\mathbf{x}_i^m - D^m(E^m(\mathbf{x}_i^m))\|_2^2. \quad (1)$$

Feature contrastive module. In the proposed framework, we distinguish between high-level and low-level features. $\{z^1, z^2, \dots, z^M\}$ are treated as low-level latent features as their diversity is retained by optimizing autoencoders. For multiple modalities, their high-level semantic should be consistent, in other words, they have the common high-level semantic. However, learning semantic consistency directly upon the latent features will destroy the diversity of multiple modalities. Accordingly, we propose a feature contrastive module $F(z_i^m; \psi_F)$, which is parameterized by ψ_F and stacked on the latent features, to learn high-level semantic features that are denoted by $\{\mathbf{h}^1, \mathbf{h}^2, \dots, \mathbf{h}^M\}$ where $\mathbf{h}_i^m \in \mathbb{R}^H$. The consistency is achieved by the following contrastive learning.

Concretely, for \mathbf{h}_i^m , there are $MN - 1$ feature pairs $\{\mathbf{h}_i^m, \mathbf{h}_j^n\}_{j=1, \dots, N}^{n=1, \dots, M}$ in total, where $\{\mathbf{h}_i^m, \mathbf{h}_i^n\}_{n \neq m}$ are regarded as $M - 1$ positive pairs and the rest $M(N - 1)$ pairs are considered as negative pairs. The similarities of positive pairs should be maximized and that of negative pairs should be minimized. To do so, the cosine distance [30, 31] is applied to measure the similarity:

$$d(\mathbf{h}_i^m, \mathbf{h}_j^n) = \frac{\langle \mathbf{h}_i^m, \mathbf{h}_j^n \rangle}{\|\mathbf{h}_i^m\| \|\mathbf{h}_j^n\|}, \quad (2)$$

where $\langle \cdot, \cdot \rangle$ is the dot product operator. Then the feature contrastive loss of the m -th modality is:

$$\mathcal{L}_{fc}^m = -\frac{1}{2N} \sum_{n \neq m} \sum_{i=1}^N \log \frac{\exp(d(\mathbf{h}_i^m, \mathbf{h}_i^n)/\tau_F)}{\sum_{j=1}^N \exp(d(\mathbf{h}_i^m, \mathbf{h}_j^n)/\tau_F) + \sum_{j=1}^N \mathbb{1}[j \neq i] \exp(d(\mathbf{h}_i^m, \mathbf{h}_j^m)/\tau_F)}, \quad (3)$$

where τ_F denotes the temperature parameter and $\mathbb{1}[\cdot]$ represents the indicator function. Considering Theorem 1, we minimize the feature contrastive loss of all modalities to learn their common high-level semantic features:

$$\mathcal{L}_{fc} = \sum_{m=1}^M \mathcal{L}_{fc}^m. \quad (4)$$

Theorem 1. *Minimizing feature contrastive loss, i.e., Eq. (4), is equivalent to maximizing mutual information among high-level features of all modalities.*

Proof. As shown in the Appendix A, the following inequality about two modalities holds:

$$-\frac{1}{N} \sum_{i=1}^N \log \frac{\exp(d(\mathbf{h}_i^m, \mathbf{h}_i^n)/\tau)}{\sum_{j=1}^N \exp(d(\mathbf{h}_i^m, \mathbf{h}_j^n)/\tau)} \geq \log N - I(\mathbf{h}^m; \mathbf{h}^n), \quad (5)$$

where $I(\mathbf{h}^m; \mathbf{h}^n)$ denotes the mutual information between \mathbf{h}^m and \mathbf{h}^n . Thus,

$$\begin{aligned} & -\frac{1}{N} \sum_{i=1}^N \log \frac{\exp(d(\mathbf{h}_i^m, \mathbf{h}_i^n)/\tau)}{\sum_{j=1}^N [\exp(d(\mathbf{h}_i^m, \mathbf{h}_j^n)/\tau) + \mathbb{1}[j \neq i] \exp(d(\mathbf{h}_i^m, \mathbf{h}_j^m)/\tau)]} \\ & \geq -\frac{1}{N} \sum_{i=1}^N \log \frac{\exp(d(\mathbf{h}_i^m, \mathbf{h}_i^n)/\tau)}{\sum_{j=1}^N \exp(d(\mathbf{h}_i^m, \mathbf{h}_j^n)/\tau)} \\ & \geq \log N - I(\mathbf{h}^m; \mathbf{h}^n). \end{aligned} \quad (6)$$

Therefore,

$$\mathcal{L}_{fc} = \sum_{m=1}^M \mathcal{L}_{fc}^m \geq \frac{1}{2} M(M-1) \log N - \sum_{m=1}^M \sum_{n=m+1}^M I(\mathbf{h}^m; \mathbf{h}^n). \quad (7)$$

Hence, minimizing Eq. (4) is equivalent to maximizing $\sum_{m=1}^M \sum_{n=m+1}^M I(\mathbf{h}^m; \mathbf{h}^n)$, i.e., the mutual information among high-level features of all modalities. \square

Label contrastive module. It is critical for multi-modal clustering to mine complementary information and obtain consistent predictions among multiple modalities. In our framework, the diversity of each modality is maintained by its low-level latent features, which are conducive to contain more complementary information. So we directly stack a label contrastive module $L(z_i^m; \psi_L)$ on the latent features to learn consistent cluster assignments, where ψ_L denotes the parameters and the last layer is set to Softmax operation. Let soft label \mathbf{Q}_{ij}^m (the output of Softmax) represent the probability that

the i -th instance belongs to the j -th cluster in the m -th modality. For M modalities, the probability of all N instances belonging to each cluster should be consistent. Therefore, we can use the above proposed contrastive learning method to achieve the consistency of multi-modal cluster predictions.

Specifically, for \mathbf{Q}_j^m , there are $MK - 1$ label pairs $\{\mathbf{Q}_{\cdot j}^m, \mathbf{Q}_{\cdot k}^n\}_{k=1, \dots, K}^{n=1, \dots, M}$ in total, where $\{\mathbf{Q}_{\cdot j}^m, \mathbf{Q}_{\cdot j}^n\}_{n \neq m}$ are constructed as $M - 1$ positive pairs and the rest $M(K - 1)$ pairs are negative pairs. For the m -th modality, we have the following label contrastive loss:

$$\mathcal{L}_{lc}^m = -\frac{1}{2K} \sum_{n \neq m} \sum_{j=1}^K \log \frac{\exp(d(\mathbf{Q}_{\cdot j}^m, \mathbf{Q}_{\cdot j}^n)/\tau_L)}{\sum_{k=1}^K \exp(d(\mathbf{Q}_{\cdot j}^m, \mathbf{Q}_{\cdot k}^n)/\tau_L) + \sum_{k=1}^K \mathbb{1}[k \neq j] \exp(d(\mathbf{Q}_{\cdot j}^m, \mathbf{Q}_{\cdot k}^m)/\tau_L)}, \quad (8)$$

where τ_L denotes the temperature parameter. Then the clustering-oriented loss function is:

$$\mathcal{L}_{lc} = \sum_{m=1}^M \mathcal{L}_{lc}^m + \sum_{m=1}^M \sum_{j=1}^K s_j^m \log s_j^m, \quad (9)$$

where $s_j^m = \frac{1}{N} \sum_{i=1}^N \mathbf{Q}_{ij}^m$. The first part of Eq. (9) aims to learn consistent clusters among all modalities. To avoid the label contrastive module from assigning all instances into a single cluster, the second part of Eq. (9), as an extra regularization term [28, 30], is also optimized to make the cluster predictions more robust. Thus, the total loss of our multi-modal contrastive learning is:

$$\mathcal{L} = \mathcal{L}_{lc} + \mathcal{L}_{fc} + \mathcal{L}_r. \quad (10)$$

3.2 Clustering with high-level semantic features

With the proposed multi-modal contrastive learning, we can obtain the high-level semantic features $\{\mathbf{h}_i^1, \mathbf{h}_i^2, \dots, \mathbf{h}_i^M\}_{i=1}^N$ and soft labels $\{\mathbf{q}_i^1, \mathbf{q}_i^2, \dots, \mathbf{q}_i^M\}_{i=1}^N$, where $\mathbf{q}_i^m = \mathbf{Q}_i^m \in \mathbb{R}^K$. In this part, we propose to take advantage of the learned high-level semantic features to fine-tune the cluster assignments. Concretely, the high-level features of all modalities are concatenated to form the global features $\mathbf{h}_i = [\mathbf{h}_i^1; \mathbf{h}_i^2; \dots; \mathbf{h}_i^M] \in \mathbb{R}^{MH}$, which are fed to K -means [17]:

$$\min_{\mathbf{c}_1, \mathbf{c}_2, \dots, \mathbf{c}_K} \sum_{i=1}^N \sum_{j=1}^K \|\mathbf{h}_i - \mathbf{c}_j\|^2, \quad (11)$$

where $\{\mathbf{c}_k\}_{k=1}^K \in \mathbb{R}^{MH}$ denote the K cluster centroids. Then, the pseudo labels of all instances $\mathbf{p} \in \mathbb{R}^N$ are obtained by:

$$\mathbf{p}_i = \operatorname{argmin}_j \|\mathbf{h}_i - \mathbf{c}_j\|^2. \quad (12)$$

Let $\tilde{\mathbf{q}}_i^m = \operatorname{argmax}_j \mathbf{q}_{ij}^m$ denote the predictions of the label contrastive module. It's worth noting that the clusters represented by \mathbf{p} and $\tilde{\mathbf{q}}^m$ are not corresponding. Therefore, we use the following maximum matching formula to calculate the modified pseudo labels for each modality:

$$\begin{aligned} \min_{\mathbf{A}^m} \sum_{i,j=1}^K \mathbf{C}_{ij}^m \mathbf{A}_{ij}^m, \quad (13) \\ \text{s.t. } \sum_{i=1}^K \mathbf{A}_{ij}^m = 1, \sum_{j=1}^K \mathbf{A}_{ij}^m = 1, \mathbf{A}_{ij}^m \in \{0, 1\}, i, j = 1, 2, \dots, K, \end{aligned}$$

where $\mathbf{A}^m \in \mathbb{R}^{K \times K}$ is the boolean matrix and $\mathbf{C}^m \in \mathbb{R}^{K \times K}$ denotes the cost matrix. $\mathbf{C}^m = \max_{i,j} \tilde{\mathbf{C}}_{ij}^m - \tilde{\mathbf{C}}^m$, where $\tilde{\mathbf{C}}_{ij}^m = \sum_{n=1}^N \mathbb{1}[\tilde{\mathbf{q}}_n^m = i] \mathbb{1}[\mathbf{p}_n = j]$. Eq. (13) can be computed efficiently by the Hungarian algorithm [36]. Thus, the modified pseudo label $\hat{\mathbf{p}}_i^m \in \mathbb{R}^K$ for the i -th instance is defined as a one-hot vector. The k -th element of $\hat{\mathbf{p}}_i^m$ is 1, where $k = k \mathbb{1}[\mathbf{A}_{ks}^m = 1] \mathbb{1}[\mathbf{p}_i = s]$, $k, s \in \{1, 2, \dots, K\}$. After that, we fine-tune the model with $\{\hat{\mathbf{p}}_i^m\}_{i=1, \dots, N}^{m=1, \dots, M}$ by cross-entropy loss:

$$\mathcal{L}_p = - \sum_{m=1}^M \sum_{i=1}^N \sum_{j=1}^K \hat{\mathbf{p}}_{ij}^m \log \mathbf{q}_{ij}^m. \quad (14)$$

Finally, the cluster prediction of the i -th instance is calculated by:

$$y_i = \operatorname{argmax}_j \left(\frac{1}{M} \sum_{m=1}^M \mathbf{q}_{ij}^m \right). \quad (15)$$

3.3 Optimization process

We adopt mini-batch gradient descent during training the model. The parameters of all networks are initialized randomly. Since the proposed learning framework aims to learn high-level semantic features from the low-level latent features, the autoencoders are pre-trained to obtain meaningful latent features to speed up model’s convergence. Then, the multi-modal contrastive learning is conducted to achieve the consistency of high-level features and cluster assignments. After pre-training and contrastive learning, the pseudo labels obtained from high-level features are modified through the maximum matching formula. The modified pseudo labels are then used to fine-tune the model. The full training process of CMMC is summarized in Algorithm 1. The obtained high-level feature extractor and label predictor can be applied to other downstream tasks.

Algorithm 1 : Contrastive Multi-Modal Clustering (CMMC)

Input:

Multi-modal dataset \mathcal{D} ; Number of clusters K ; Temperature parameters τ_F and τ_L ; The number of epochs for pre-training E_p , multi-modal contrastive learning E_c , and fine-tuning E_f .

Output:

The high-level feature extractor $\{\{\theta^m\}_{m=1}^M, \psi_F\}$; The label predictor $\{\{\theta^m\}_{m=1}^M, \psi_L\}$.

- 1: Initialize the network parameters of autoencoders $\{\theta^m, \phi^m\}_{m=1}^M$, feature contrastive module ψ_F , and label contrastive module ψ_L .
 - 2: **for** $epoch = 1$ to E_p **do**
 - 3: Pre-train $\{\theta^m, \phi^m\}_{m=1}^M$ by minimizing Eq. (1).
 - 4: **for** $epoch = 1$ to E_c **do**
 - 5: Update $\psi_F, \psi_L, \{\theta^m, \phi^m\}_{m=1}^M$ by minimizing Eq. (10).
 - 6: Compute global clusters and pseudo labels by Eqs. (11) and (12).
 - 7: Maximum matching pseudo labels by solving Eq. (13).
 - 8: **for** $epoch = 1$ to E_f **do**
 - 9: Fine-tune $\psi_L, \{\theta^m\}_{m=1}^M$ by minimizing Eq. (14).
 - 10: Calculate cluster predictions by Eq. (15).
-

Let n represent the batch size and D denote the maximum number of neurons in hidden layers of neural networks. As the mini-batch gradient descent is adopted, the complexity to train the model is $O(N/n(n^3M^2 + K^3M^2 + nMK + nMD^2))$ that is linear to data size N . So CMMC can be easily applied to large-scale data tasks. The detailed complexity analysis is shown in the Appendix B.

4 Experiments

4.1 Experimental setup

Datasets. The experiments are carried out on the following popular datasets. **BDGP** [37] contains 2,500 examples of drosophila embryos, each of which is represented by visual and textual features. **MNIST-USPS** [19] is a popular handwritten digit (0-9) dataset, which contains 5,000 examples provided with two modalities of digital images. **CCV** (Columbia Consumer Video) [38] is a video dataset with 6,773 examples belonging to 20 classes, which provides hand-crafted Bag-of-Words (BoW) representations of three modalities, including STIP, SIFT, and MFCC. **Fashion** [39] is an image dataset about products, such as Coat, Dress, and T-shirt, etc. We use 30,000 images to construct a three-modal version, where each instance consists of three different images that belong to the same class. In this way, the three modalities of each instance are the same products with three styles. **Caltech** [40], a RGB image dataset, provides five modalities including WM, CENTRIST, LBP, GIST, and HOG features. We adopt 7 classes (each class contains 200 instances) and build four datasets based on the five modalities for evaluating the scalability of the multi-modal clustering methods.

Baseline models. The following popular and state-of-the-art clustering algorithms are chosen as baselines. **K -means** [17] is one of the most widely used methods. **DEC** [41] is the most popular deep embedded clustering method. K -means and DEC are both single-modal (or single-view) clustering methods. **BMVC** [42] handles multi-view clustering with binary learning. **RMSL** [12] is a subspace

The details of the complexity analysis, complete proofs, used datasets, network structures, and parameter settings are provided in the Appendix.

Table 1: Quantitative comparison results. Bold denotes the best results and underline denotes the second-best.

Datasets	BDGP			MNIST-USPS			CCV			Fashion		
Metrics	ACC	NMI	Purity									
<i>K</i> -means (1967)	0.432	0.569	0.740	0.768	0.723	0.768	0.123	0.057	0.134	0.709	0.656	0.713
DEC (2016)	0.946	0.881	0.946	0.731	0.715	0.757	0.194	0.189	0.210	0.674	0.725	0.696
BMVC (2018)	0.422	0.153	0.428	0.885	0.886	0.886	0.171	0.134	0.204	<u>0.795</u>	0.767	0.814
RMSL (2019)	0.849	0.630	0.849	0.424	0.318	0.428	0.215	0.157	0.243	0.408	0.405	0.421
MVC-LFA (2019)	0.564	0.395	0.612	0.768	0.675	0.768	0.232	0.195	0.261	0.791	0.759	0.794
COMIC (2019)	0.578	0.642	0.639	0.482	0.709	0.531	0.104	0.000	0.104	0.578	0.642	0.608
DAMC* (2019)	<u>0.982</u>	<u>0.946</u>	<u>0.982</u>	N/A	N/A	N/A	0.256	0.225	<u>0.286</u>	N/A	N/A	N/A
EAMC* (2020)	N/A	N/A	N/A	N/A	N/A	N/A	<u>0.261</u>	<u>0.266</u>	0.271	N/A	N/A	N/A
SAMVC (2020)	0.556	0.456	0.573	0.669	0.727	0.725	0.136	0.077	0.148	0.615	0.684	0.652
DEMVC (2021)	0.954	0.887	0.955	<u>0.978</u>	<u>0.973</u>	<u>0.978</u>	0.238	0.242	0.273	0.792	<u>0.901</u>	0.796
CMMC (ours)	0.989	0.966	0.989	0.995	0.985	0.995	0.300	0.271	0.330	0.992	0.980	0.992

Table 2: The performance on Caltech with scalable modalities. “-*X*M” represents there are *X* modalities.

Datasets	Caltech-2M			Caltech-3M			Caltech-4M			Caltech-5M		
Metrics	ACC	NMI	Purity									
BMVC (2018)	0.666	<u>0.475</u>	<u>0.579</u>	0.514	0.462	0.560	0.634	0.537	0.671	<u>0.743</u>	<u>0.676</u>	<u>0.766</u>
RMSL (2019)	0.525	0.474	0.540	<u>0.554</u>	<u>0.480</u>	0.554	0.596	0.551	0.608	0.354	0.340	0.391
MVC-LFA (2019)	0.462	0.348	0.496	0.551	<u>0.423</u>	<u>0.578</u>	0.609	0.522	0.636	0.741	0.601	0.747
COMIC (2019)	0.188	0.147	0.241	0.155	0.134	0.231	0.451	0.573	0.811	0.156	0.111	0.211
SAMVC (2020)	0.507	0.412	0.529	0.530	0.478	0.559	0.559	0.512	0.585	0.648	0.591	0.668
DEMVC (2021)	0.497	0.404	0.519	0.526	0.411	0.540	<u>0.635</u>	<u>0.601</u>	0.646	0.711	0.671	0.729
CMMC (ours)	<u>0.590</u>	0.507	0.593	0.614	0.561	0.619	0.688	0.636	<u>0.691</u>	0.777	0.699	0.777

learning based multi-view clustering method. **MVC-LFA** [43] performs multi-view clustering with the proposed late fusion alignment maximization. **COMIC** [19] presents a clustering framework by matching cross views. **DAMC** [7] is a deep multi-view clustering method with adversarial training. **EAMC** [10] proposes an adversarial-attention network for multi-modal clustering. **SAMVC** [44] is an auto-weighted method combined with self-paced learning. **DEMVC** [20] extends the deep embedded clustering to deal with multi-modal (or multi-view) clustering tasks.

Implementation details. Considering generality, the same neural network architecture is used for all datasets in CMMC. Concretely, for all modalities, the autoencoders are fully connected neural networks with the same structure. The feature and label contrastive modules are implemented with Multi-Layer Perceptrons (MLPs). The activation function is Rectified Linear Unit (ReLU) and the last layer of the label contrastive module is Softmax.

Evaluation metrics. The clustering performance is evaluated by three metrics, including clustering accuracy (ACC), normalized mutual information (NMI), and Purity. For all of these metrics, a higher value denotes better performance. The mean values of ten independent runs are reported.

4.2 Comparisons with state of the arts

The quantitative comparison results are shown in Table 1. The results of the methods marked with * are excerpted from [7, 10]. There are eleven clustering methods including shallow models (*K*-means, BMVC, RMSL, MVC-LFA, COMIC, and SAMVC) and deep models (DEC, DAMC, EAMC, DEMVC, and CMMC). It can be seen that the clustering performance obtained by multi-modal methods generally surpasses that by the single-modal methods (i.e., *K*-means and DEC), which indicates that the multi-modal clustering methods can utilize the complementary information contained in multiple modalities more effectively. Compared with the above ten clustering methods, our CMMC achieves state-of-the-art clustering performance. Especially for CCV and Fashion, CMMC outperforms them by a large margin. The pivotal reason is, by our proposed multi-modal contrastive learning, CMMC can mine the high-level semantic features to improve clustering performance.

Interestingly, for MNIST-USPS and Fashion, the modalities are different in styles but belong to the same class, so that the high-level semantic of multiple modalities is highly consistent. Since our method emphasizes learning the high-level semantic, it can obtain almost accurate cluster predictions. For CCV, the performance remains limited even though we have achieved the best results. This can

be attributed to the three hand-crafted modalities (i.e., STIP, SIFT, and MFCC) are not necessarily consistent in terms of the high-level semantic and cluster information of video data.

4.3 Performance on scalable modalities

On Caltech, we build four datasets to test the scalability of the multi-modal clustering methods. Specifically, Caltech-2M has two modalities including WM and CENTRIST. Compared with Caltech-2M, Caltech-3M adds LBP, Caltech-4M adds LBP and GIST. Caltech-5M includes WM, CENTRIST, LBP, GIST, and HOG. Table 2 shows the comparisons, from which we could have two conclusions: (1) The clustering performance of the methods is generally improved with the increase of the number of modalities. (2) Our approach mostly achieves the best performance regardless of how many modalities the dataset contains. Consequently, the conclusions have verified CMMC’s scalability and its capability to mine multi-modal complementary information to improve clustering performance.

5 Model analysis

5.1 Ablation studies

Table 3: Ablation studies on BDGP and MNIST-USPS.

	Components of CMMC	BDGP			MNIST-USPS		
		ACC	NMI	Purity	ACC	NMI	Purity
(1)	\mathcal{L}_{lc}	0.624	0.595	0.636	0.913	0.912	0.913
(2)	$\mathcal{L}_{lc} + \mathcal{L}_{fc}$	0.812	0.746	0.816	0.961	0.951	0.967
(3)	$\mathcal{L}_{lc} + \mathcal{L}_{fc} + \mathcal{L}_r$	0.975	0.939	0.975	0.984	0.974	0.984
(4)	$\mathcal{L}_{lc} + \mathcal{L}_{fc} + \mathcal{L}_r$ and \mathcal{L}_p	0.989	0.966	0.989	0.995	0.985	0.995

We conduct ablation studies with four variants of CMMC to show the effectiveness of its different components. (1) We only use the label contrastive module to learn consistent cluster predictions of multiple modalities. (2) Feature contrastive module is added to learn common high-level semantic features of all modalities. (3) The reconstruction of autoencoders is optimized to maintain the multi-modal diversity among the low-level latent features. (4) Compared with setting “(3)”, we additionally fine-tune the cluster predictions with the pseudo labels generated from global high-level semantic features. Table 3 shows the loss components and experimental results corresponding to the four variants. Significantly, one can find that each component of CMMC has improved the clustering performance, which further proves the effectiveness of our motivations and the proposed framework.

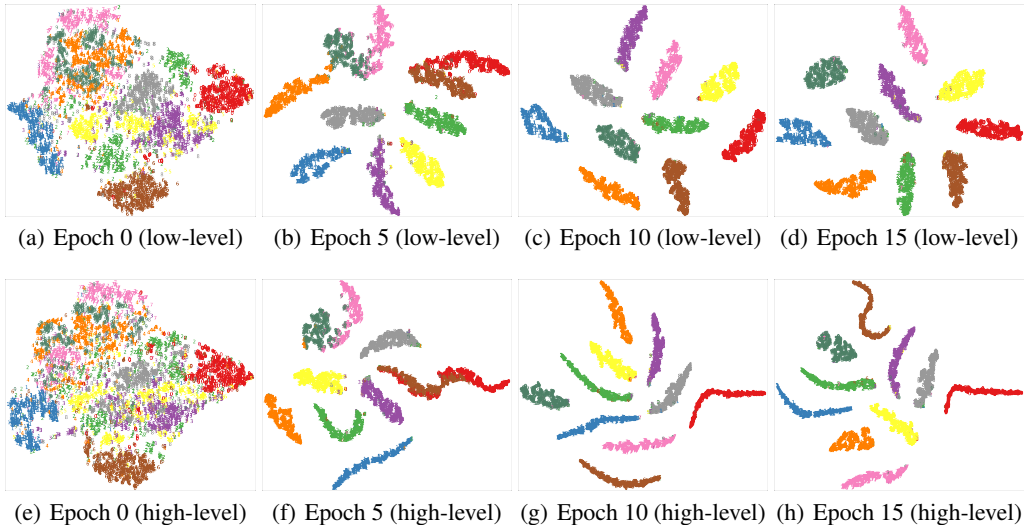


Figure 2: Visualization of low-level latent features (a-d) and high-level semantic features (e-h) during training.

5.2 Visualization

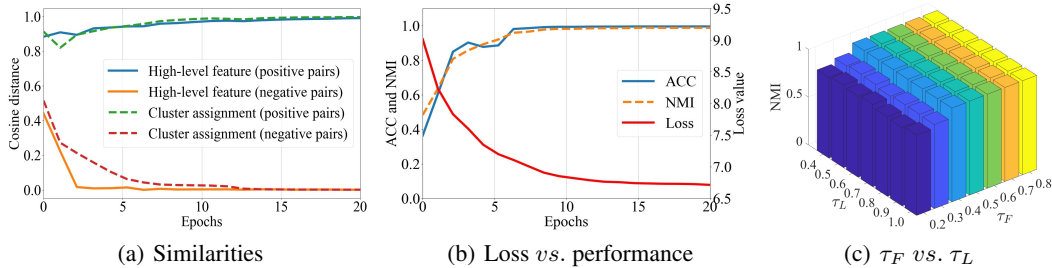


Figure 3: (a) The similarities of feature and label pairs during contrastive learning. (b) Clustering and convergence performance. (c) Hyperparameters sensitivity analysis.

To verify the mechanism of the proposed model, in Figures 2 and 3, we take MNIST-USPS as an example and visualize its learning process. The learned features of MNIST are shown in Figure 2 via t -SNE [45]. It can be discovered that the cluster structures of low-level and high-level features become clear and clear during the proposed multi-modal contrastive learning. The clusters of low-level features are sparse as they keep the diversity among each other. Interestingly, compared with the clusters of low-level features, that of high-level features are denser, which learns better low-dimensional manifolds and indicates that high-level semantic information is mined. Besides, in Figure 3(a), the similarities of positive feature and label pairs are rising while that of negative feature and label pairs are decreasing. Meanwhile, as shown in Figure 3(b), the clustering performance improves with the decrease of loss values. In consequence, these observations verify the mechanism of our framework. That is, it can achieve the consistency of high-level features and cluster predictions while maintaining the diversity of multiple modalities, which creates a positive feedback in improving the clustering performance.

Convergence and sensitivity analysis. The training error shown in Figure 3(b) indicates that CMMC enjoys good convergence property. In addition, the hyperparameters of CMMC include the temperature parameters τ_F and τ_L corresponding to the feature and label contrastive modules. Figure 3(c) shows the mean NMI values of ten independent runs, which indicates that our framework is insensitive to the choice of τ_F and τ_L . Empirically, we let $\tau_F = 0.5$ and $\tau_L = 1.0$ for all datasets.

6 Conclusion

In this paper, we have proposed contrastive multi-modal clustering (CMMC). Specially, we distinguish between low-level features and high-level features in a novel multi-modal contrastive learning paradigm. In the proposed framework, for multiple modalities, their diversity is maintained in the low-level features via optimizing autoencoders. The feature and label contrastive modules learn multi-modal common high-level semantic features and consistent cluster assignments, respectively. To leverage the high-level semantic features for multi-modal clustering, we solve a maximum matching problem to generate pseudo labels, which are further used to fine-tune the model. Extensive experiments on different datasets demonstrate that CMMC has good scalability and achieves state-of-the-art clustering performance.

Except for the fundamental task (i.e., multi-modal clustering) in this work, the proposed framework can learn exquisite representations. Therefore, the learned high-level feature extractor and label predictor can be applied to more downstream tasks, such as classification, image segmentation, anomaly detection, and cross-modal retrieval, etc. However, this work aims to provide a general framework and it might be affected by the intrinsic bias of data especially with dirty instances in other applications. For example, it may not work when the multiple modalities of data do not have consistent or common high-level semantic. Thus, our future work will focus on eliminating the disturbances caused by data bias and generalize our framework to more application scenarios.

Acknowledgment

This work was supported in part by National Natural Science Foundation of China (No. 61806043), and Sichuan Science and Technology Program (Nos. 2021YFS0172 and 2020YFS0119).

References

- [1] Tadas Baltrušaitis, Chaitanya Ahuja, and Louis-Philippe Morency. Multimodal machine learning: A survey and taxonomy. *TPAMI*, 41(2):423–443, 2018. 1
- [2] Liang Peng, Yang Yang, Zheng Wang, Zi Huang, and Heng Tao Shen. Mra-net: Improving vqa via multi-modal relation attention network. *TPAMI*, 2020. 1
- [3] Xiaofeng Zhu, Xuelong Li, and Shichao Zhang. Block-row sparse multiview multilabel learning for image classification. *IEEE transactions on cybernetics*, 46(2):450–461, 2015. 1
- [4] Raed Saqur and Karthik Narasimhan. Multimodal graph networks for compositional generalization in visual question answering. *NeurIPS*, pages 3070–3081, 2020. 1
- [5] Yuki M Asano, Mandela Patrick, Christian Rupprecht, and Andrea Vedaldi. Labelling unlabelled videos from scratch with multi-modal self-supervision. *NeurIPS*, pages 4660–4671, 2020. 1
- [6] Feiping Nie, Jing Li, and Xuelong Li. Self-weighted multiview clustering with multiple graphs. In *IJCAI*, pages 2564–2570, 2017. 1, 3
- [7] Zhaoyang Li, Qianqian Wang, Zhiqiang Tao, Quanxue Gao, and Zhaohua Yang. Deep adversarial multi-view clustering network. In *IJCAI*, pages 2952–2958, 2019. 1, 3, 7
- [8] Mahdi Abavisani and Vishal M Patel. Deep multimodal subspace clustering networks. *JSTSP*, 12(6):1601–1614, 2018. 1, 3
- [9] Di Hu, Feiping Nie, and Xuelong Li. Deep multimodal clustering for unsupervised audiovisual learning. In *CVPR*, pages 9248–9257, 2019. 1, 3
- [10] Runwu Zhou and Yi-Dong Shen. End-to-end adversarial-attention network for multi-modal clustering. In *CVPR*, pages 14619–14628, 2020. 1, 3, 7
- [11] Tao Zhou, Changqing Zhang, Xi Peng, Harish Bhaskar, and Jie Yang. Dual shared-specific multiview subspace clustering. *IEEE transactions on cybernetics*, 50(8):3517–3530, 2019. 1
- [12] Ruihuang Li, Changqing Zhang, Huazhu Fu, Xi Peng, Tianyi Zhou, and Qinghua Hu. Reciprocal multi-layer subspace learning for multi-view clustering. In *ICCV*, pages 8172–8180, 2019. 1, 6, 15
- [13] Qinghai Zheng, Jihua Zhu, Zhongyu Li, Shanmin Pang, Jun Wang, and Yaochen Li. Feature concatenation multi-view subspace clustering. *Neurocomputing*, 379:89–102, 2020. 1
- [14] Jialu Liu, Chi Wang, Jing Gao, and Jiawei Han. Multi-view clustering via joint nonnegative matrix factorization. In *SDM*, pages 252–260, 2013. 1
- [15] Handong Zhao, Zhengming Ding, and Yun Fu. Multi-view clustering via deep matrix factorization. In *AAAI*, pages 2921–2927, 2017. 1
- [16] Zuyuan Yang, Naiyao Liang, Wei Yan, Zhenni Li, and Shengli Xie. Uniform distribution non-negative matrix factorization for multiview clustering. *IEEE transactions on cybernetics*, pages 3249–3262, 2021. 1
- [17] James MacQueen. Some methods for classification and analysis of multivariate observations. In *Proceedings of the 5th Berkeley Symposium on Mathematical Statistics and Probability*, pages 281–297, 1967. 1, 5, 6, 15
- [18] Kun Zhan, Changqing Zhang, Junpeng Guan, and Junsheng Wang. Graph learning for multiview clustering. *IEEE transactions on cybernetics*, 48(10):2887–2895, 2017. 1, 3
- [19] Xi Peng, Zhenyu Huang, Jiancheng Lv, Hongyuan Zhu, and Joey Tianyi Zhou. COMIC: Multi-view clustering without parameter selection. In *ICML*, pages 5092–5101, 2019. 1, 3, 6, 7, 14, 15
- [20] Jie Xu, Yazhou Ren, Guofeng Li, Lili Pan, Ce Zhu, and Zenglin Xu. Deep embedded multi-view clustering with collaborative training. *Information Sciences*, 2021. 1, 3, 7, 15

- [21] Jie Xu, Yazhou Ren, Huayi Tang, Zhimeng Yang, Lili Pan, Yang Yang, and Xiaorong Pu. Self-supervised discriminative feature learning for multi-view clustering. *arXiv preprint arXiv:2103.15069*, 2021. 1, 3
- [22] Humam Alwassel, Dhruv Mahajan, Bruno Korbar, Lorenzo Torresani, Bernard Ghanem, and Du Tran. Self-supervised learning by cross-modal audio-video clustering. *NeurIPS*, pages 9758–9770, 2019. 1
- [23] Xiaochun Cao, Changqing Zhang, Huazhu Fu, Si Liu, and Hua Zhang. Diversity-induced multi-view subspace clustering. In *CVPR*, pages 586–594, 2015. 2
- [24] Shirui Luo, Changqing Zhang, Wei Zhang, and Xiaochun Cao. Consistent and specific multi-view subspace clustering. In *AAAI*, 2018. 3
- [25] Xiao Cai, Feiping Nie, and Heng Huang. Multi-view k-means clustering on big data. In *IJCAI*, pages 2598–2604, 2013. 3
- [26] Yoshua Bengio, Aaron Courville, and Pascal Vincent. Representation learning: A review and new perspectives. *TPAMI*, 35(8):1798–1828, 2013. 3
- [27] Ting Chen, Simon Kornblith, Mohammad Norouzi, and Geoffrey Hinton. A simple framework for contrastive learning of visual representations. In *ICML*, pages 1597–1607, 2020. 3
- [28] Wouter Van Gansbeke, Simon Vandenhende, Stamatios Georgoulis, Marc Proesmans, and Luc Van Gool. Scan: Learning to classify images without labels. In *ECCV*, pages 268–285, 2020. 3, 5
- [29] Chuang Niu and Ge Wang. Spice: Semantic pseudo-labeling for image clustering. *arXiv preprint arXiv:2103.09382*, 2021. 3
- [30] Yunfan Li, Peng Hu, Zitao Liu, Dezhong Peng, Joey Tianyi Zhou, and Xi Peng. Contrastive clustering. *AAAI*, 2021. 3, 4, 5
- [31] Yonglong Tian, Dilip Krishnan, and Phillip Isola. Contrastive multiview coding. *ECCV*, pages 776–794, 2020. 3, 4
- [32] Kaveh Hassani and Amir Hosein Khasahmadi. Contrastive multi-view representation learning on graphs. In *ICML*, pages 4116–4126, 2020. 3
- [33] Yijie Lin, Yuanbiao Gou, Zitao Liu, Boyun Li, Jiancheng Lv, and Xi Peng. Completer: Incomplete multi-view clustering via contrastive prediction. In *CVPR*, 2021. 3
- [34] Nicolas Pielawski, Elisabeth Wetzter, Johan Öfverstedt, Jiahao Lu, Carolina Wählby, Joakim Lindblad, and Nataša Sladoje. Comir: Contrastive multimodal image representation for registration. *NeurIPS*, pages 18433–18444, 2020. 3
- [35] Geoffrey E Hinton and Ruslan R Salakhutdinov. Reducing the dimensionality of data with neural networks. *Science*, 313(5786):504–507, 2006. 3
- [36] Roy Jonker and Ton Volgenant. Improving the hungarian assignment algorithm. *Operations Research Letters*, 5(4):171–175, 1986. 5, 14
- [37] Xiao Cai, Hua Wang, Heng Huang, and Chris Ding. Joint stage recognition and anatomical annotation of drosophila gene expression patterns. *Bioinformatics*, 28(12):i16–i24, 2012. 6, 14
- [38] Yu-Gang Jiang, Guangnan Ye, Shih-Fu Chang, Daniel Ellis, and Alexander C Loui. Consumer video understanding: A benchmark database and an evaluation of human and machine performance. In *Proceedings of the 1st ACM International Conference on Multimedia Retrieval*, pages 1–8, 2011. 6, 14
- [39] Han Xiao, Kashif Rasul, and Roland Vollgraf. Fashion-mnist: a novel image dataset for benchmarking machine learning algorithms. *CoRR*, 2017. 6, 14
- [40] Li Fei-Fei, Rob Fergus, and Pietro Perona. Learning generative visual models from few training examples: An incremental bayesian approach tested on 101 object categories. In *CVPR*, pages 178–178, 2004. 6, 14
- [41] Junyuan Xie, Ross Girshick, and Ali Farhadi. Unsupervised deep embedding for clustering analysis. In *ICML*, pages 478–487, 2016. 6, 15
- [42] Zheng Zhang, Li Liu, Fumin Shen, Heng Tao Shen, and Ling Shao. Binary multi-view clustering. *TPAMI*, 41(7):1774–1782, 2018. 6, 15

- [43] Siwei Wang, Xinwang Liu, En Zhu, Chang Tang, Jiyuan Liu, Jingtao Hu, Jingyuan Xia, and Jianping Yin. Multi-view clustering via late fusion alignment maximization. In *IJCAI*, pages 3778–3784, 2019. 7, 15
- [44] Yazhou Ren, Shudong Huang, Peng Zhao, Minghao Han, and Zenglin Xu. Self-paced and auto-weighted multi-view clustering. *Neurocomputing*, 383:248–256, 2020. 7, 15
- [45] Laurens van der Maaten and Geoffrey Hinton. Visualizing data using t-sne. *JMLR*, 9:2579–2605, 2008. 9
- [46] Aaron van den Oord, Yazhe Li, and Oriol Vinyals. Representation learning with contrastive predictive coding. *arXiv preprint arXiv:1807.03748*, 2018. 13, 14
- [47] Huasong Zhong, Chong Chen, Zhongming Jin, and Xian-Sheng Hua. Deep robust clustering by contrastive learning. *arXiv preprint arXiv:2008.03030*, 2020. 13
- [48] David McAllester and Karl Stratos. Formal limitations on the measurement of mutual information. In *International Conference on Artificial Intelligence and Statistics*, pages 875–884. PMLR, 2020. 14
- [49] Adam Paszke, Sam Gross, Francisco Massa, Adam Lerer, James Bradbury, Gregory Chanan, Trevor Killeen, Zeming Lin, Natalia Gimelshein, Luca Antiga, et al. Pytorch: An imperative style, high-performance deep learning library. *NeurIPS*, pages 8024–8035, 2019. 15

Appendix A Proof of theorem

Let m and n denote two modalities, we prove the following theorem:

Theorem 1. *The following inequality holds:*

$$-\frac{1}{N} \sum_{i=1}^N \log \frac{\exp(d(\mathbf{h}_i^m, \mathbf{h}_i^n)/\tau)}{\sum_{j=1}^N \exp(d(\mathbf{h}_i^m, \mathbf{h}_j^n)/\tau)} \geq \log N - I(\mathbf{h}^m; \mathbf{h}^n). \quad (16)$$

First, we give the next lemma.

Lemma 1. *The optimal value of $\exp(d(\mathbf{h}^m, \mathbf{h}^n)/\tau)$ is proportional to the ratio of $p(\mathbf{h}^m, \mathbf{h}^n)$ to $p(\mathbf{h}^m)p(\mathbf{h}^n)$, i.e., $\exp(d(\mathbf{h}^m, \mathbf{h}^n)/\tau) \propto \frac{p(\mathbf{h}^m, \mathbf{h}^n)}{p(\mathbf{h}^m)p(\mathbf{h}^n)}$.*

Proof. Let \mathcal{L}_c denote the contrastive loss, i.e.,

$$\mathcal{L}_c = -\frac{1}{N} \sum_{i=1}^N \log \frac{\exp(d(\mathbf{h}_i^m, \mathbf{h}_i^n)/\tau)}{\sum_{j=1}^N \exp(d(\mathbf{h}_i^m, \mathbf{h}_j^n)/\tau)} \quad (17)$$

Eq. (17) can be regarded as a cross-entropy loss. Thus, minimizing this loss is equivalent to solving a binary classification problem, namely, classifying the given pairs into positive or negative pairs. Let $\{\mathbf{h}_i^m, \mathbf{h}_i^n\}$ denote the positive pairs and $\{\mathbf{h}_i^m, \mathbf{h}_j^n\}_{j \neq i}$ denote the negative pairs. For each given pairs $\{\mathbf{h}_i^m, \mathbf{h}_j^n\}_{i,j=1}^N$, let $p(\mathbf{h}_i^n | \{\mathbf{h}_1^m, \dots, \mathbf{h}_N^m\}, \mathbf{h}_i^m)$ denote the predicted probability of finding \mathbf{h}_i^n from $\{\mathbf{h}_1^m, \dots, \mathbf{h}_N^m\}$ to form positive pairs $\{\mathbf{h}_i^m, \mathbf{h}_i^n\}$. $p(\mathbf{h}^m, \mathbf{h}^n)$, $p(\mathbf{h}^m)$, and $p(\mathbf{h}^n)$ denote the joint probability and marginal probabilities of \mathbf{h}^m and \mathbf{h}^n . Then, the optimal value of $p(\mathbf{h}_i^n | \{\mathbf{h}_1^m, \dots, \mathbf{h}_N^m\}, \mathbf{h}_i^m)$ is:

$$\begin{aligned} p(\mathbf{h}_i^n | \{\mathbf{h}_1^m, \dots, \mathbf{h}_N^m\}, \mathbf{h}_i^m) &= \frac{p(\mathbf{h}_i^n | \mathbf{h}_i^m) \prod_{l \neq i} p(\mathbf{h}_l^n)}{\sum_{j=1}^N p(\mathbf{h}_j^n | \mathbf{h}_i^m) \prod_{l \neq j} p(\mathbf{h}_l^n)} \\ &= \frac{\frac{p(\mathbf{h}_i^n | \mathbf{h}_i^m)}{p(\mathbf{h}_i^n)}}{\sum_{j=1}^N \frac{p(\mathbf{h}_j^n | \mathbf{h}_i^m)}{p(\mathbf{h}_j^n)}} \\ &= \frac{\frac{p(\mathbf{h}_i^m, \mathbf{h}_i^n)}{p(\mathbf{h}_i^m)p(\mathbf{h}_i^n)}}{\sum_{j=1}^N \frac{p(\mathbf{h}_i^m, \mathbf{h}_j^n)}{p(\mathbf{h}_i^m)p(\mathbf{h}_j^n)}}. \end{aligned} \quad (18)$$

The corresponding cross-entropy loss is:

$$\mathcal{L} = -\frac{1}{N} \sum_{i=1}^N \log p(\mathbf{h}_i^n | \{\mathbf{h}_1^n, \dots, \mathbf{h}_N^n\}, \mathbf{h}_i^m) = -\frac{1}{N} \sum_{i=1}^N \log \frac{\frac{p(\mathbf{h}_i^m, \mathbf{h}_i^n)}{p(\mathbf{h}_i^m)p(\mathbf{h}_i^n)}}{\sum_{j=1}^N \frac{p(\mathbf{h}_i^m, \mathbf{h}_j^n)}{p(\mathbf{h}_i^m)p(\mathbf{h}_j^n)}}. \quad (19)$$

Comparing Eq. (19) with Eq. (17), we can find $\exp(d(\mathbf{h}^m, \mathbf{h}^n)/\tau) \propto \frac{p(\mathbf{h}^m, \mathbf{h}^n)}{p(\mathbf{h}^m)p(\mathbf{h}^n)}$. \square

When $j \neq i$, we assume that $p(\mathbf{h}_i^m, \mathbf{h}_j^n) = p(\mathbf{h}_i^m)p(\mathbf{h}_j^n)$. Thus, $p(\mathbf{h}_j^n | \mathbf{h}_i^m) = \frac{p(\mathbf{h}_j^n, \mathbf{h}_i^m)}{p(\mathbf{h}_i^m)} = p(\mathbf{h}_j^n)$ if $j \neq i$. We further prove Theorem 1.

Proof. Let $\mathcal{S}_i = \sum_{j=1}^N \frac{p(\mathbf{h}_i^m, \mathbf{h}_j^n)}{p(\mathbf{h}_i^m)p(\mathbf{h}_j^n)}$, therefore,

$$\begin{aligned} I(\mathbf{h}^m; \mathbf{h}^n) &= \sum_{i=1}^N \sum_{j=1}^N p(\mathbf{h}_i^m, \mathbf{h}_j^n) \log \frac{p(\mathbf{h}_i^m, \mathbf{h}_j^n)}{p(\mathbf{h}_i^m)p(\mathbf{h}_j^n)} \\ &= \sum_{i=1}^N \sum_{j=1}^N p(\mathbf{h}_i^m, \mathbf{h}_j^n) \log \left(\frac{p(\mathbf{h}_i^m, \mathbf{h}_j^n)}{p(\mathbf{h}_i^m)p(\mathbf{h}_j^n) \mathcal{S}_i} \right) \\ &= \sum_{i=1}^N \sum_{j=1}^N p(\mathbf{h}_i^m, \mathbf{h}_j^n) \log \frac{\frac{p(\mathbf{h}_i^m, \mathbf{h}_j^n)}{p(\mathbf{h}_i^m)p(\mathbf{h}_j^n)}}{\mathcal{S}_i} + \sum_{i=1}^N \sum_{j=1}^N p(\mathbf{h}_i^m, \mathbf{h}_j^n) \log \mathcal{S}_i \\ &= \sum_{i=1}^N p(\mathbf{h}_i^m, \mathbf{h}_i^n) \log \frac{\frac{p(\mathbf{h}_i^m, \mathbf{h}_i^n)}{p(\mathbf{h}_i^m)p(\mathbf{h}_i^n)}}{\mathcal{S}_i} + \sum_{i=1}^N \sum_{j \neq i} p(\mathbf{h}_i^m, \mathbf{h}_j^n) \log \frac{\frac{p(\mathbf{h}_i^m, \mathbf{h}_j^n)}{p(\mathbf{h}_i^m)p(\mathbf{h}_j^n)}}{\mathcal{S}_i} \\ &\quad + \sum_{i=1}^N \sum_{j=1}^N p(\mathbf{h}_i^m, \mathbf{h}_j^n) \log \mathcal{S}_i. \\ &= \sum_{i=1}^N p(\mathbf{h}_i^m, \mathbf{h}_i^n) \log \frac{\frac{p(\mathbf{h}_i^m, \mathbf{h}_i^n)}{p(\mathbf{h}_i^m)p(\mathbf{h}_i^n)}}{\mathcal{S}_i} + \sum_{i=1}^N \sum_{j \neq i} p(\mathbf{h}_i^m, \mathbf{h}_j^n) \log \frac{p(\mathbf{h}_i^m)p(\mathbf{h}_j^n)}{p(\mathbf{h}_i^m)p(\mathbf{h}_j^n)} \\ &\quad + \sum_{i=1}^N \sum_{j=1}^N p(\mathbf{h}_i^m, \mathbf{h}_j^n) \log \mathcal{S}_i - \sum_{i=1}^N \sum_{j \neq i} p(\mathbf{h}_i^m, \mathbf{h}_j^n) \log \mathcal{S}_i \\ &= \sum_{i=1}^N p(\mathbf{h}_i^m, \mathbf{h}_i^n) \log \frac{\frac{p(\mathbf{h}_i^m, \mathbf{h}_i^n)}{p(\mathbf{h}_i^m)p(\mathbf{h}_i^n)}}{\mathcal{S}_i} + \sum_{i=1}^N p(\mathbf{h}_i^m, \mathbf{h}_i^n) \log \mathcal{S}_i. \end{aligned} \quad (20)$$

Since positive pairs are correlated, we have the estimate: $p(\mathbf{h}_i^m, \mathbf{h}_i^n) \geq p(\mathbf{h}_i^m)p(\mathbf{h}_i^n)$. Therefore, the following inequality holds:

$$\begin{aligned} \log \mathcal{S}_i &= \log \left(\sum_{j=1}^N \frac{p(\mathbf{h}_i^m, \mathbf{h}_j^n)}{p(\mathbf{h}_i^m)p(\mathbf{h}_j^n)} \right) \\ &= \log \left(\frac{p(\mathbf{h}_i^m, \mathbf{h}_i^n)}{p(\mathbf{h}_i^m)p(\mathbf{h}_i^n)} + \sum_{j \neq i} \frac{p(\mathbf{h}_i^m, \mathbf{h}_j^n)}{p(\mathbf{h}_i^m)p(\mathbf{h}_j^n)} \right) \\ &= \log \left(N + \frac{p(\mathbf{h}_i^m, \mathbf{h}_i^n)}{p(\mathbf{h}_i^m)p(\mathbf{h}_i^n)} - 1 \right) \\ &\geq \log N. \end{aligned} \quad (21)$$

According to Lemma 1 and Eq. (21), we assume that there exists a constant $\delta \in (0, 1)$ such that $p(\mathbf{h}_i^m | \mathbf{h}_i^n) \geq \delta, i = 1, 2, \dots, N$ holds. With the estimation [46, 47], i.e., $p(\mathbf{h}_i^n) \approx \frac{1}{N}, i =$

1, 2, \dots , N , the following inequality holds:

$$\begin{aligned}
I(\mathbf{h}^m; \mathbf{h}^n) &= \sum_{i=1}^N p(\mathbf{h}_i^m, \mathbf{h}_i^n) \log \frac{p(\mathbf{h}_i^m, \mathbf{h}_i^n)}{p(\mathbf{h}_i^m)p(\mathbf{h}_i^n)} + \sum_{i=1}^N p(\mathbf{h}_i^m, \mathbf{h}_i^n) \log \mathcal{S}_i \\
&\approx \sum_{i=1}^N \frac{1}{N} p(\mathbf{h}_i^m | \mathbf{h}_i^n) \log \frac{p(\mathbf{h}_i^m, \mathbf{h}_i^n)}{p(\mathbf{h}_i^m)p(\mathbf{h}_i^n)} + \sum_{i=1}^N \frac{1}{N} p(\mathbf{h}_i^m | \mathbf{h}_i^n) \log \mathcal{S}_i \\
&\geq \delta \left(\frac{1}{N} \sum_{i=1}^N \log \frac{\exp(d(\mathbf{h}_i^m, \mathbf{h}_i^n)/\tau)}{\sum_{j=1}^N \exp(d(\mathbf{h}_i^m, \mathbf{h}_j^n)/\tau)} + \log N \right).
\end{aligned} \tag{22}$$

Further,

$$-\frac{1}{N} \sum_{i=1}^N \log \frac{\exp(d(\mathbf{h}_i^m, \mathbf{h}_i^n)/\tau)}{\sum_{j=1}^N \exp(d(\mathbf{h}_i^m, \mathbf{h}_j^n)/\tau)} \geq \log N - \frac{1}{\delta} I(\mathbf{h}^m; \mathbf{h}^n). \tag{23}$$

Consequently, when the constant $\delta \approx 1$ (i.e., the positive pairs are correlated), Theorem 1 holds. \square

According to [46], Eq. (23) is more precise when N is larger. Minimizing the left part of Eq. (23) is equivalent to maximizing the mutual information $I(\mathbf{h}^m; \mathbf{h}^n)$. Note that this bound is weak as there exists approximation about mutual information [48].

Appendix B Complexity analysis

Let N, M, K represent the data size, the number of modalities, and the number of clusters, respectively. Let D denote the maximum number of neurons in hidden layers of deep neural networks. H denotes the dimensionality of high-level features. n is the batch size. Generally $N \gg M, K, D, H, n$ holds. In the mini-batch optimization process, it is not difficult to find that the complexity to compute the reconstruction loss, feature contrastive loss, label contrastive loss, and cross-entropy loss is $O(nM)$, $O(n^3M^2)$, $O(K^3M^2 + nMK)$, and $O(nMK)$, respectively. The complexity of deep neural networks is $O(nMD^2)$. Therefore, the total complexity to train the model is $O(N/n(n^3M^2 + K^3M^2 + nMK + nMD^2))$, which is linear to N . In addition, the complexity of K -means is $O(NMHK)$. For all modalities, the complexity of using Hungarian algorithm [36] is $O(MK^3)$. In conclusion, the complexity of CMMC is linear to the data size N which can be easily applied to large-scale data tasks.

Appendix C Datasets

We carry out the experiments on the following five popular datasets. **BDGP** [37] contains 2500 examples about drosophila embryos, each of which is represented by a 1750-dim visual feature and a 79-dim textual feature. **MNIST-USPS** [19] is a popular handwritten digit (0-9) dataset, which contains 5000 examples provided with two modalities of digital images. **CCV** (Columbia Consumer Video) [38] is a video dataset with 6773 examples belonging to 20 classes, which provides hand-crafted Bag-of-Words (BoW) representations of three modalities, including 5000-dim STIP, 5000-dim SIFT, and 4000-dim MFCC. **Fashion** [39] is an image dataset about products, such as Coat, Dress, and T-shirt, etc. We use 30000 images to construct a three-modal version, where each instance consists of three different images that belong to the same class. In this way, the three modalities of each instance are the same products with three styles. **Caltech** [40], a RGB image dataset, provides five modalities including 40-dim wavelet moments (WM), 254-dim CENTRIST, 928-dim LBP, 512-dim GIST, and 1984-dim HOG. We adopt 200 instances from each class and 1400 instances in total for evaluating the scalability of the multi-modal clustering methods. Concretely, based on the five modalities, we build four datasets containing Caltech-2M, Caltech-3M, Caltech-4M, and Caltech-5M, where “-XM” represents there are X modalities. Table 4 presents a summary of datasets used in our experiments.

Table 4: The description of datasets.

Dataset	type	#sample	#modality	#class
BDGP	image, text	2,500	2	5
MNIST-USPS	digit of different styles	5,000	2	10
CCV	video (STIP, SIFT, MFCC)	6,773	3	20
Fashion	product of different styles	10,000	3	10
Caltech-2M	WM, CENTRIST	1,400	2	7
Caltech-3M	WM, CENTRIST, LBP	1,400	3	7
Caltech-4M	WM, CENTRIST, LBP, GIST	1,400	4	7
Caltech-5M	WM, CENTRIST, LBP, GIST, HOG	1,400	5	7

Appendix D Experimental settings

CMMC. In the proposed model, fully connected network with the same architecture is adopted as the autoencoder to learn low-level latent features. Concretely, for each modality, the encoder is: Input – 500 – 500 – 2000 – 512 and the decoder is 512 – 2000 – 500 – 500 – Output. All the input data is reshaped into vectors. The feature and label contrastive modules are implemented by Multi-Layer Perceptrons (MLPs) with dimensions of 512 – 512 – 128 and 512 – 512 – K , respectively, where K is the number of classes. The temperature parameters of feature and label contrastive modules are empirically set to 0.5 and 1, respectively. Adam optimizer with a learning rate of 0.0003 is adopted in optimization. The batch size is 256. For all datasets, the epoch of pre-training E_p is 200. For the datasets with different data scale, the required epochs E_c of multi-modal contrastive learning should be different. In the experiments, E_c is empirically set to 10, 50, 50, 50 and 100 on BDGP, MNIST-USPS, CCV, Caltech and Fashion, respectively. The fine-tuning epoch E_f is set to 30 on all datasets.

The proposed CMMC model is implemented in PyTorch [49] and the code is provided in the supplemental material. All the experiments are conducted on a linux PC with GeForce GTX 1080Ti (10G) GPU and Intel(R) Core(TM) i7-6800K CPU @ 3.40GHz.

Comparing methods. For all comparing methods, the released codes and the optimal hyper-parameter settings recommended by authors are adopted. To be specific, the trade-off coefficient γ in DEMVC [20] is 0.1. For BMVC [42], r , β , γ , λ , and the code length are 5, 0.003, 0.01, 10^{-5} and 128, respectively. For COMIC [19], the neighbor size is set to 10 and $\epsilon^{(v)}$ is set to 0.9. For SAMVC [44], the SPL controlling parameter $\lambda^{(v)}$ is 0.15. In MVC-LFA [43], Gaussian kernel is adopted and λ is 8. For RMSL [12], the trade-off parameters α and β are 0.4 and 0.7, respectively. The dimensionality of K is 200. The regularization parameter γ is 0.1. As K -means [17] and DEC [41] can not deal with multi-modal clustering tasks, we concatenate all modalities’ data as their inputs for comparisons. In addition, since the complexity of RMSL is too high, i.e., $O(N^3)$, the data of CCV and Fashion are split into two equal parts to test the algorithm.